A Modified Algorithm for the Simulation of Charge Behavior in Water Tree Aged Cross-Linked Polyethylene Cable

YU ZHANG[ID], DEYUAN LIU, JIANDONG WU, (Member, IEEE), AND YI YIN, (Member, IEEE)

School of Electronic Information and Electrical Engineering, Shanghai Jiao Tong University, Shanghai 200240, China

Corresponding author: Jiandong Wu (jdwu@sjtu.edu.cn)

ABSTRACT In this paper, a modified algorithm is introduced to explain the process of charge formation in water tree aged cable insulation with respect to the dielectric properties of water tree areas and the cylindrical geometries of cable insulation. The algorithm combined with the classic bipolar charge transport model represents a novel attempt to simulate charge behavior in insulation with water tree. The finite-difference method is employed to solve for the electric field in the presence of space charge, and the finite-volume method is employed to solve the charge continuity equation. The dielectric parameters in this paper are not instantaneous near the interface but are functions of the radius. To overcome the Courant–Friedrichs–Lewy condition, the Crank–Nicolson method is used to separate the governing equations in the time domain. To validate the accuracy of the model, this paper also presents the space charge behavior in water tree aged cross-linked polyethylene cable samples measured by the full-scale pulsed electro-acoustic method. The homocharge is injected under a high electric field. During the depolarization process, the shallow trap charge gradually disappears, whereas the homocharge continues to form a positive peak signal. Simulations show that the homocharge accumulates in the tip of the water tree because the dielectric characteristics of the material change during the water-aging process. The model describes the behavior of space charge in the water tree aged insulation of cylindrical geometries. Improvements will be needed in the following research.

INDEX TERMS Water tree, XLPE, space charge, Crank-Nicolson, bipolar charge transport model, cable insulation, algorithm design and analysis.

I. INTRODUCTION

In recent years, cross-linked polyethylene (XLPE) cable has come into wide use in urban power grids due to its high reliability, ease of installation, and excellent electrical and thermal properties [1]. Although XLPE cable has many advantages over other types of cable, such as oil-filled cable, it also has its own challenges. Some unavoidable defects occur during power operation, and these may distort the original electric field distribution, leading to the development of more serious defects and finally to insulation degradation or even insulation failure [2], [3]. Among the unstable factors, water tree degradation, which occurs commonly in underground XLPE-insulated cables, is one of the most serious. Because water tree degradation poses a serious threat to the stable operation of power grids, many studies of water tree detection have been conducted [4], [5]. Most of the detection methods used in these studies, including the power frequency

method, damped AC, very low frequency (VLF), dielectric spectroscopy, and depolarization current, measure changes in dielectric loss and permittivity [6]–[10]. These methods are designed primarily to evaluate the entire cable insulation rather than to precisely determine the fault location, which is the main objective of other classes of measuring techniques, such as time-domain reflectometry methods [11]. However, none of these measuring techniques can be used to detect the locations of water trees in the radial direction. Currently, space charge measurement is popular as a method of testing the status of insulation through the distribution of space charge, which actually reflects the distribution of traps or defects. In recent years, the relationship between space charge and the location of water trees has also received attention [12]–[16]. Li *et al.* [12] measured the space charge distribution at any phase angle of the applied ac voltage and proved that PEA method could be a nondestructive method

for evaluating water tree length. Suzuki *et al.* [13] found that there is a rule correspondence between space charge and water tree position. Thomas and Saha [14], [15] developed a new dielectric response model for water tree degraded XLPE insulation, who found that mechanical linearity or non-linearity mechanism based upon the observed structure of water trees consisting of voids with interlinking channels concern space charge behavior. Hui *et al.* [16] measured the space charge distribution in XLPE/silica nanocomposites and found that total charge accumulated in the water tree area consists of the injected charges from the electrodes and the trapped water ions. However, the existing researches on space charge in water tree-degraded insulation are primarily experimental. Studies that focus on the algorithm improvement in simulation of charge transport in solid dielectrics need to be carried out more; since simulations are essential to explain the charge formation procedure and could provide a new reference for charge simulation in solid dielectrics containing defects.

Many researchers are interested in investigating charge behavior in solid dielectrics via simulation [17]–[19]. Most papers in this area have concentrated on space charge behaviors in a single dielectric or in two dielectrics with characteristics that do not differ widely. In solid dielectrics, the bipolar charge transport model originally proposed by Alison and Hill [17] is quite popular for charge transport simulation, including charge injection, transport, trapping, and recombination. The governing equations of the model are based on the law of conservation of mass. Through decades of development, the bipolar charge transport model has been gradually improved and expanded by many researchers. Roy *et al.* [18] adopted the model to study the space charge behavior in a single solid dielectric in detail, both in plates and in dielectrics with coaxial geometry. Lan [19] studied heterocharge accumulation in XLPE, including the behavior of ionic charges due to the dissociation of impurities, using a modified bipolar charge transport model. In those models, the algorithm time-step for solving the charge conservation equation is limited by the Courant-Friedrichs-Lewy (CFL) condition. Because the conductivity of the solid dielectrics that these investigators are interested in is very small, the CFL requirement for an acceptable mesh and time-step is easily satisfied; however, when considering the space charge simulation in the water tree zone, the CFL condition is not easily satisfied. According to previous research [20], the conductivity in the water tree is almost 10 orders of magnitude greater than that found in XLPE insulation. On the macroscopic scale, it is found that there is a decay of void and channel density near the water tree tip, leading to a change in conductivity and permittivity that is not instantaneous but diffuse.

To overcome the limitations of previous works, we investigated space charge behavior by introducing a new algorithm and a new distribution of dielectric parameters for water tree-degraded XLPE cables. The overall goal of this work is to expand the application range of the bipolar charge

transport model to better describe space charge behavior in the insulation used in practical engineering, including insulation that may suffer from water tree degradation and other defects. In this paper, simulated and experimental results are compared and verified.

In the simulation, the finite difference method (FDM) and the finite volume method are adopted to iteratively solve the Poisson and charge conservation equations. In the time domain, the Crank-Nicolson method is introduced to separate the governing equations and to overcome the time-step limitation. To describe the diffuse distributions of permittivity and conductivity near the interface, the dielectric parameters in this paper are not instantaneous but are functions of the radius. In the experiments, a modified pulsed electro-acoustic (PEA) measurement system designed for cable insulation is employed to measure the space charge distribution in water-aged XLPE cable; the details of the system are presented in [21].

II. SIMULATION
A. THE MODIFIED BIPOLAR CHARGE TRANSPORT MODEL
The base component, i.e., the law of charge generation and extraction, of the simulation follows a modified bipolar charge transport model with respect to the formation and transport of ionic charges [19], [22]. To contrapuntally simulate the injected charge accumulation at the tree region near both sides of the cable insulation, only generation, transport, trapping, detrapping, recombination, and extraction of electrons and holes are included in the model presented in this paper; the behavior of ionic charges is ignored to avoid the disturbance these charges introduce in the calculation of the location and amount of the injected charges. The simulation model in this paper is modified in the following ways: with regard to cylindrical geometry in governing equations, the conductivity and permittivity are functions of the radius and the Crank-Nicolson method is adopted in the time domain to overcome the time-step limitation. The changes in the parameters due to the presence of certain conditions in the insulation are described in the section titled *Dielectric Parameters*. Other details of the parameters used in this model are presented in the section titled *Parameters of the Modified Bipolar Charge Transport Model*.

B. CHARGE GENERATION
In this model, the generation of holes and electrons at the electrodes follows Schottky's law, which can be stated as follows:

$$\begin{cases} j_h(R_0+L, t) = AT^2 \exp(-\frac{ew_{hi}}{kT}) \exp(\frac{e}{kT}\sqrt{\frac{eE(R_0+L, t)}{4\pi\varepsilon(R_0+L, t)}}) \\ j_e(R_0, t) = AT^2 \exp(-\frac{ew_{ei}}{kT}) \exp(\frac{e}{kT}\sqrt{\frac{eE(R_0, t)}{4\pi\varepsilon(R_0, t)}}) \end{cases}$$
(1)

where $j_h(R_0 + L, t)$ and $j_e(R_0, t)$ are the injection current densities at the anode and the cathode, respectively; $E(R_0 + L, t)$ and $E(R_0, t)$ are the local electric fields at the

anode and the cathode, respectively; A is the Richardson constant; T is the temperature; e is the elementary electronic charge; k is the Boltzmann constant; w_{hi} and w_{ei} are the injection barrier heights for holes and electrons, respectively; and $\varepsilon(R_0+L, t)$ and $\varepsilon(R_0, t)$ are the permittivities at the anode and the cathode, respectively.

C. GOVERNING EQUATIONS
Poisson's equation in cylindrical coordinates:

$$\frac{1}{r}\frac{\partial}{\partial r}\left(-\varepsilon r\frac{\partial \varphi}{\partial r}\right) = \rho \quad (2)$$

Charge conservation equation:

$$\frac{\partial n_a}{\partial t} + \nabla \cdot j_a = s_a \quad (3)$$

The current densities satisfy $j_a = \mu_a n_a E$ where r is the distance to the center of the conductor, φ is the electric potential, ρ is the density of net charge, ε is the permittivity, n is the density of charge, $\nabla\cdot$ is the divergence, j is the current density, s is the generation of particles per unit volume per unit time, μ is the mobility, E is the electric field, and the index a refers to the type of particle (h for holes and e for electrons).

D. CHARGE EXTRACTION
Both holes and electrons will be partially blocked when transported to the opposite interface; this is described as follows:

$$\begin{cases} j_h(R_0, t) = C_h \cdot \mu_h(R_0, t) \cdot n_h(R_0, t) \cdot E(R_0, t) \\ j_e(R_0+L, t) = C_e \cdot \mu_e(R_0+L, t) \cdot n_e(R_0+L, t) \cdot E(R_0+L, t) \end{cases}$$
$$(4)$$

where $j_h(R_0, t)$ and $j_e(R_0 + L, t)$ are the extraction current densities for holes and electrons at the cathode and anode, respectively, and C_h and C_e are the extraction coefficients for holes and electrons, respectively; C_h and C_e vary from 0 to 1.

E. DIELECTRIC PARAMETERS
Considering the particularity of the interface of the water tree and the XLPE insulation, which is not ideally instantaneous, the space charge process cannot be considered via a simple Maxwell-Wagner interfacial model. According to the definition used to describe the interface, there are innumerable interfaces between the water tree and the XLPE insulation because the dielectric parameters are diffusely distributed near the water tree tip.

In both the water tree and the XLPE insulation, the dielectric characteristics can be regarded as uniform with increased distance from the water tree tip. The manner of mathematically describing the transition from the water tree to the XLPE insulation, which is essential for solving the governing equations, is important. To obtain the exact form of permittivity and conductivity by measurement is impossible as of the writing of this paper. The assumptions used in the simulation are either based on available references that have been

verified or were indirectly verified later by comparison of the simulation results and the experimental results.

Based on the above-mentioned reasons, A. J. Thomas proposed a new dielectric response model for water tree-degraded XLPE insulation [14], [15]. However, the space charge behavior of the electrode/XLPE interface, which is a theoretical limitation for space charge behavior simulation near the electrode, is neglected in Thomas' model. In the bipolar charge transport model, both injection and extraction of electrons and holes are considered.

The conductivity and permittivity near the water tree are assumed to change in an exponential manner in reference to Thomas' model [14], [15], which has a physical background and has been verified in similar areas. The conductivity and permittivity can be written as follows:

$$\sigma(r) = \frac{\sigma_m}{1+e^{\alpha(r-l)}} + \frac{\sigma_w}{1+e^{-\alpha(r-l)}} \quad (5)$$

$$\varepsilon(r) = \frac{\varepsilon_m}{1+e^{\alpha(r-l)}} + \frac{\varepsilon_w}{1+e^{-\alpha(r-l)}} \quad (6)$$

where r is the distance to the center of the conductor; σ_m and ε_m are the XLPE conductivity and permittivity, respectively; σ_w and ε_w are the water tree conductivity and permittivity, respectively; the indexes m and w refer to healthy XLPE material and to the water tree, respectively; the conductivity satisfies $\sigma = \mu n$; α is a shape parameter; and l is a location parameter determining the spatial location in the r-direction of the uniform XLPE electrical properties. Note that the water tree in this paper is a vented tree.

F. PARAMETERS OF THE MODIFIED BIPOLAR CHARGE TRANSPORT MODEL
Previous experiments [13], [23] presented the reasons for believing that charge injection between an electrode and a water tree is easier than charge injection between an electrode and healthy XLPE insulation. Thus, in this paper, the injection barrier height of holes is set to be lower than that of the electrons. The remaining parameterization of the model refers to the values from our previous works [19]. The parameters used in this paper are listed in Table 1.

G. MODIFIED ALGORITHM DESCRIPTION
Considering the asymmetry of the cable geometry and the boundary condition, a simulation is conducted in one dimension only. Poisson's equation is solved using the FDM.

Solving the charge conservation equation in the time domain is the most important problem in this algorithm. By adopting Green's formula and integrating (3) in the *ith* element, the following equation can be obtained:

$$\int_{L_i} \frac{\partial n_a(r_i, t)}{\partial t} dl = -(j_a(r_{i+\frac{1}{2}}, t) - j_a(r_{i-\frac{1}{2}}, t))$$
$$+ \int_{L_i} s_a(r_i, t) dl \quad (7)$$

where L_i is the length of the *ith* element, $i + \frac{1}{2}$ represents the middle point of the *ith* and *i+1th* elements, and $i - \frac{1}{2}$

TABLE 1. Parameters used in the simulation.

Parameter	Value	Unit
T	300	K
w_{hi}	1.24	eV
w_{ei}	1.27	eV
ε_w	3	1
ε_m	2.3	1
σ_w	1×10^{-7}	S/m
σ_m	1×10^{-17}	S/m
μ_{hm}	$1 \times 10^{-6} \exp(-0.54e/kT)$	$m^2 \cdot V^{-1} \cdot s^{-1}$
μ_{em}	$2.6 \times 10^{-6} \exp(-0.54e/kT)$	$m^2 \cdot V^{-1} \cdot s^{-1}$
k	1.38×10^{-23}	$J \cdot K^{-1}$
C_h	0.8	1
C_e	0.8	1
α	10^6	m^{-1}
S	4×10^{-3}	$m^3 \cdot C^{-1} \cdot s^{-1}$
l	3×10^{-4}	m

represents the middle point of the *ith* and *i-1th* elements. Note that the source term, $s_a(r_i, t)$, in this paper is assumed to be influenced only by the combination of electrons and holes that satisfies the equation $s_a(r_i, t) = -Sn_u(r_i, t)n_h(r_i, t)$, where S is the combination parameter. The equation shows that influences such as the trapping process and the detrapping process are neglected.

The charge density n_a is assumed to be uniformly distributed within each element. Thus, (7) can be written as follows:

$$\frac{\partial n_a(r_i, t)}{\partial t} L_i = -((\mu_a n_a(r_{i+\frac{1}{2}}, t)E(r_{i+\frac{1}{2}}, t)$$
$$- (\mu_a n_a(r_{i-\frac{1}{2}}, t)E(r_{i-\frac{1}{2}}, t))) + s_a(r_i, t)L_i \quad (8)$$

The first-order upwind method is adopted to calculate the space charge of the edge point $n_a(r_{i+\frac{1}{2}}, t)$ and $n_a(r_{i-\frac{1}{2}}, t)$. For the electric field of the edge point, a conventional interpolation method is adopted to calculate the electric field of an arbitrary point.

To speed up calculation of the non-linear problem of (8), the Strang splitting method is used to decouple (8) into two independent equations, as follows [24]:

$$\begin{cases} \dfrac{\partial n_a(r_i, t)}{\partial t} L_i = s_a(r_i, t)L_i \\ \dfrac{\partial n_a(r_i, t)}{\partial t} L_i = -((\mu_a n_a(r_{i+\frac{1}{2}}, t)E(r_{i+\frac{1}{2}}, t) \\ \qquad - (\mu_a n_a(r_{i-\frac{1}{2}}, t)E(r_{i-\frac{1}{2}}, t))) \end{cases} \quad (9)$$

To overcome the time-step limitation, the Crank-Nicolson method is adopted in the time domain. According to the

Crank-Nicolson method [25],

$$\frac{\partial n_a(r_i, t)}{\partial t} = \frac{n_a(r_i, t + \Delta t) - n_a(r_i, t)}{\Delta t} \quad (10)$$

$$n_a(r_i, t) = \frac{1}{2}(n_a(r_i, t + \Delta t) + n_a(r_i, t)) \quad (11)$$

Substituting (10) and (11) in (9), only electrons and holes are considered. The time-domain form can then be written as follows:

$$\begin{cases} \dfrac{n_{u(i)}^{j+1} - n_{u(i)}^{j}}{\Delta t} = -S\dfrac{1}{2}(n_{u(i)}^{j+1} + n_{u(i)}^{j})\dfrac{1}{2}(n_{p(i)}^{j+1} + n_{p(i)}^{j}) \\ \dfrac{n_{p(i)}^{j+1} - n_{p(i)}^{j}}{\Delta t} = -S\dfrac{1}{2}(n_{u(i)}^{j+1} + n_{u(i)}^{j})\dfrac{1}{2}(n_{p(i)}^{j+1} + n_{p(i)}^{j}) \end{cases} \quad (12)$$

$$\begin{cases} \dfrac{n_{u(i)}^{j+1} - n_{u(i)}^{j}}{\Delta t} = -\dfrac{1}{L_i}(\mu_u E_{i+\frac{1}{2}}^{j}\dfrac{1}{2}(n_{u(i)}^{j+1} + n_{u(i)}^{j}) \\ \qquad - (\mu_u E_{i-\frac{1}{2}}^{j}\dfrac{1}{2}(n_{u(i-1)}^{j+1} + n_{u(i-1)}^{j}))) \\ \dfrac{n_{h(i)}^{j+1} - n_{h(i)}^{j}}{\Delta t} = -\dfrac{1}{L_i}(\mu_h E_{i+\frac{1}{2}}^{j}\dfrac{1}{2}(n_{h(i+1)}^{j+1} + n_{h(i+1)}^{j}) \\ \qquad - (\mu_h E_{i-\frac{1}{2}}^{j}\dfrac{1}{2}(n_{h(i)}^{j+1} + n_{h(i)}^{j}))) \end{cases} \quad (13)$$

According to the Strang splitting method, the calculation is divided into three steps:
1) Take $n_{u(i)}^{j}$ and $n_{p(i)}^{j}$ as the initial values, and take $\frac{1}{2}\Delta t$ as the time-step to solve (12); the transition values $n_{u(i)}^{j^1}$ and $n_{p(i)}^{j^1}$ can be obtained.
2) Take $n_{u(i)}^{j^1}$ and $n_{p(i)}^{j^1}$ as the initial values, and take Δt as the time-step to solve (13); the transition values $n_{u(i)}^{j^2}$ and $n_{p(i)}^{j^2}$ can be obtained.
3) Take $n_{u(i)}^{j^2}$ and $n_{p(i)}^{j^2}$ as the initial values, and take $\frac{1}{2}\Delta t$ as the time-step to solve (12); the next time-step values $n_{u(i)}^{j+1}$ and $n_{p(i)}^{j+1}$ can be obtained.

In the initial time, it is assumed that the net charge in the insulation is zero. Thus the Poisson equation could be solved by FDM. The boundary conditions when solving the Poisson equation at each time step are voltages that applied to the electrodes. For the continuity condition, the permittivity and potential are linear interpolated within each element in the simulation, which is reasonable when the values of adjacent elements are similar. This results in the continuity condition $\varepsilon_1 \frac{\partial \varphi_1}{\partial n_1} = \varepsilon_2 \frac{\partial \varphi_2}{\partial n_2}$ always satisfied in this paper.

III. EXPERIMENTS
A. SAMPLE PREPARATION
XLPE cables with a rated voltage of 8.7/10 kV (U_0/U) were prepared. U_0 is the rated power-frequency voltage between the conductor and an earth metallic screen, and U is the rated power-frequency voltage between conductors of different phases. The thickness of the cable insulation is approximately 4.5 mm. The cables were aged using both electric and thermal stresses to simulate practical operating conditions. An AC

current was applied to the conductors to obtain a conductor temperature of 90 °C for the cables. During the entire heating period, $2U_0$ with frequency of 50 *Hz* was applied between the conductor and the metal screen. The cables were divided into two groups; the water tree aged cables were aged in tap water at room temperature for 6 months, and the cables used for comparison were not aged in tap water.

B. SPACE CHARGE MEASUREMENT

The schematic diagram of the PEA measurement system for cylindrical geometry is shown in Fig. 1 [21]. The DC voltage is applied to the conductor directly and the pulse voltage is applied to the conductor through a capacitor. The inner and outer electrodes are semi-conductive material.
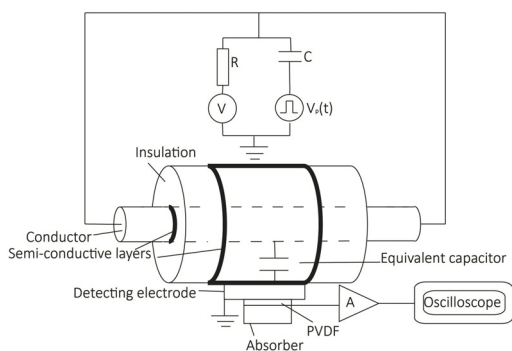
**FIGURE 1.** The schematic diagram of the PEA measurement system for cylindrical geometry.

In order to study the injected charge behavior in water tree area, it should be calculated whether voltage applied to the sample is enough to trigger charge injection. In the initial state, it could be assumed that there is no charge in the insulation. Thus it could be considered as Laplace field at the beginning. The electric field can be calculated by:

$$E = -\nabla\varphi = \frac{U}{rIn(R_2/R_1)}. \tag{14}$$

where U is applied voltage, R_1 is the radius of cathode, R_2 is the radius of anode, r is the radius. When the average electric field is 10 kV/mm, the electric field at both anode and cathode of the model in this paper could be estimated, which are 7.88 kV/mm and 13 kV/mm respectively. According to previous researches [13], [23], the threshold of electric field for charge injection between water tree and electrode is surely under 7 kV/mm. 8-10 kV/mm is the threshold of electric field for charge injection between XLPE insulation and electrode according to previous researches [26], [27].

The voltage application process during space charge measurement is shown in Fig. 2.

For each measurement, a negative DC field of 3 kV/mm was applied for 5 min as a reference electric field. A negative DC field of 10 kV/mm was then applied for 30 min, followed by the application of fields of 15 and 20 kV/mm for 30 min. Finally, the two electrodes were short-circuited for 30 min. The space charge distribution was recorded for each cable at
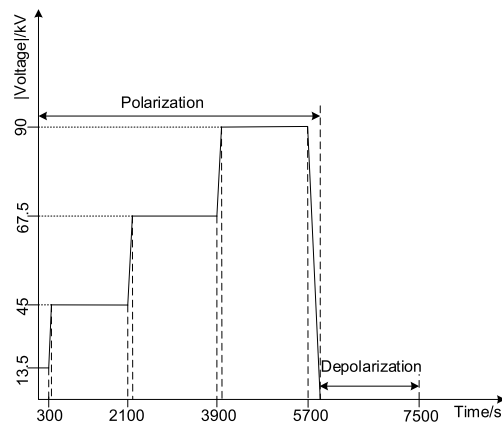
FIGURE 2. Schematic diagram showing the voltage application process during space charge measurement.

various times with the field applied and under short-circuit conditions.

C. WATER TREE OBSERVATION

To retain the cable samples in as close to their original state as possible, the water tree aging process imitates practical conditions. Thus, the conventional accelerated water tree aging method in which a metal needle is used to produce pinhole defects in the XLPE samples is not adopted. Cable samples must be sliced to determine whether a water tree actually exists at the measurement point after PEA measurement. To find a vented tree at the measurement point is not an easy task. For this reason, there are actually no trees at the measurement point in some of the cable samples in which the PEA waveform is considered to indicate a vented tree.

In this study, 32 cable samples were measured using the PEA method. For each sample, the insulation at the measurement point opposite the transducer was radially sliced into transverse samples approximately $200\mu m$ in width for water tree observation.

The slices were stained in methylene blue solution (the temperature of which was maintained at 90 °C) for 60 minutes. The methylene blue solution was made up of two solutions: A, 5*g* methylene blue and 1000*mL* distilled water; B, 4*gNaOH* and 100*mL* distilled water. The slices were examined microscopically for the presence of water trees at 200x magnification.

IV. RESULTS
A. EXPERIMENTAL RESULTS
The space charge data were directly acquired during the polarization and depolarization process. To accurately investigate the charge behavior in the area of the vented tree in which the voltage signal is near the signal of the capacitive charge at the anode, the capacitive charge signal is removed; otherwise, the charge signal of the vented tree will be obscured by the large capacitive charge signal. The data obtained during the depolarization process are then

considered; however, fast mobile charges may not be captured during this period. According to a previous study [27], a subtraction method is proposed to overcome the limitations of the above two methods. This method provides a more intuitive view of the charge behavior inside the insulation when voltage is applied. Furthermore, eliminating the capacitive charge but retaining the fast mobile charges is also consistent with the physical process of the simulation model presented in this paper.

Mathematically, the subtraction method can be expressed as follows:

$$\rho_{acc}(x) = \rho_{app}(x) - \frac{V_{app}}{V_{ref}}\rho_{ref}(x) \qquad (15)$$

where $\rho_{acc}(x)$ represents the space charge density after subtraction; $\rho_{app}(x)$ and $\rho_{ref}(x)$ represent the charge densities at the applied voltage and the reference voltage, respectively; and V_{ref} and V_{app} denote the reference voltage and the applied voltage, respectively.

The results of the water tree observations indicated that 3 cable samples are well matched; this means that vented trees exist in the insulation of the corresponding PEA measurement points. The PEA measured waveforms of the 3 selected water tree aged cables and the 3 compared unaged cables, as well as the water tree images are sufficient to validate the accuracy of the model presented in this paper.

The space charge distribution of unaged and water-aged cables during the polarization and depolarization processes were measured. (15) is applied to the data obtained for the polarization process. The study of this paper focus on the area near the anode electrode, which is marked by a dotted rectangle in Fig. 3, 4 and 5.

Note that since the space charge in the water tree area mainly accumulates at the water tree tip, the material that the acoustic signal passes through when propagating to the transducer is still XLPE. Thus, the attenuation factor used in the post-processing program refers to the attenuation factor of XLPE.

Fig. 3 shows the space charge distribution during the polarization. The "A" of "AU" and "AW" indicates that the cables were obtained from manufacturer A; "U" indicates that the cable is unaged, and "W" indicates that the cable is water-aged. "BU," "BW," "CU," and "CW" can be understood in the same manner. In group A and B, heterocharge indicated by labels "1" and "3" are found near the anode. Charge "1" and "3" are thought from field-assisted ionic dissociation of chemical species intrinsic to the insulation. Compared with unaged cables, homocharge "2" and "5" are obviously present near the anode in the water-aged cables in groups A and C. In group B, homocharge "4" could reluctantly be seen in the water-aged cable. Compared with group A and C, the difference in the charge distribution near the anode between the unaged and water-aged cables in group B is not very obvious from observation of the original data obtained during the polarization process. Besides, the
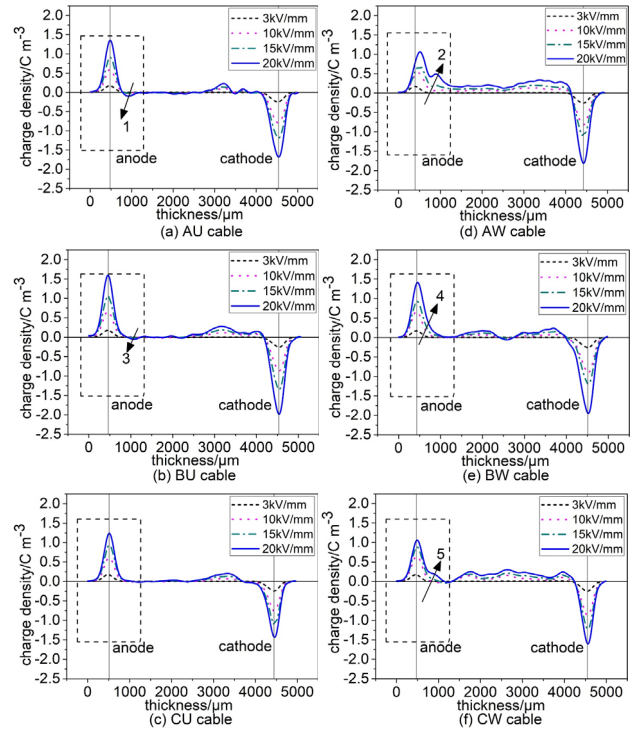

FIGURE 3. Space charge distribution of unaged (a, b, c) and water-aged (d, e, f) cables during the polarization process.
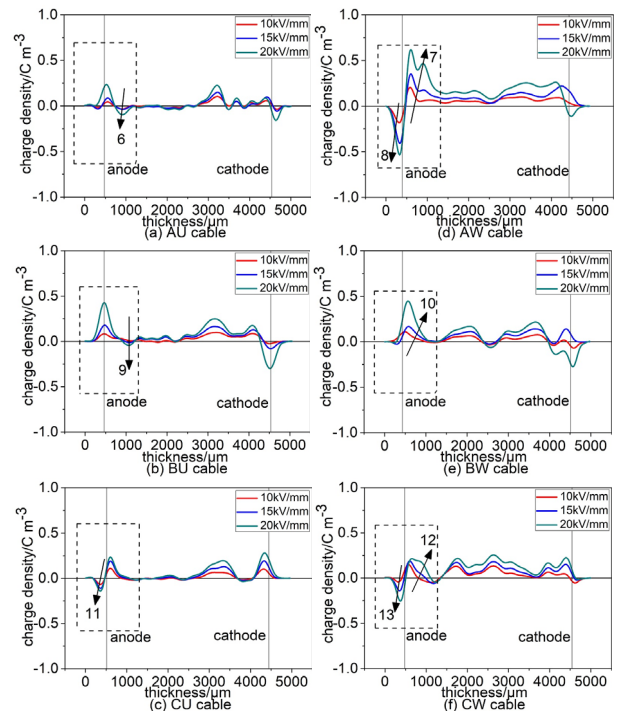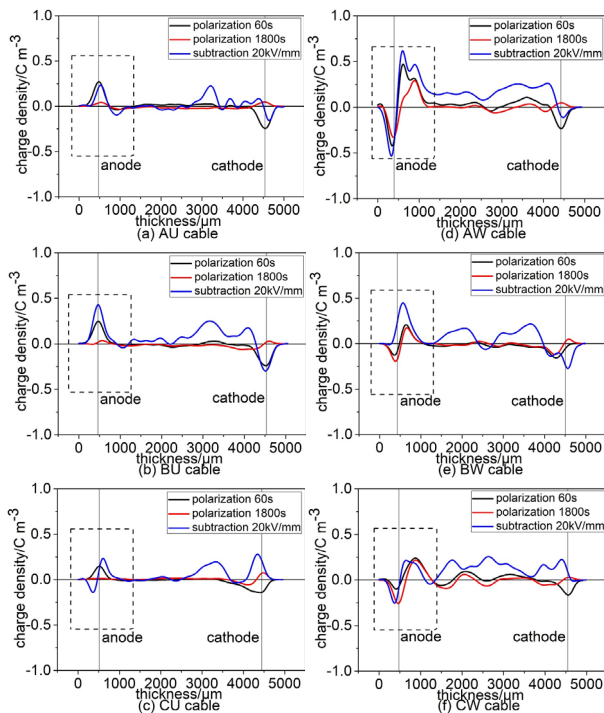

FIGURE 4. Space charge distribution of unaged (a, b, c) and water-aged (d, e, f) cables determined using the subtraction method with the polarization process data.

amplitude of induced charge peaks in anode is found smaller for water-aged cables among all groups.

Fig. 4 shows the space charge distribution of unaged and water-aged cables after the application of the subtraction

method to the polarization process data. After the elimination of the capacitive charge, the homocharge "7," "10" and "12" near the anode are more obvious than they are in the original data indicated by labels "2," "4" and "5" obtained during the polarization process, indicating that the water tree exists. The length of water tree along radial direction can be estimated according to the position of homocharge peak. Once the length of water tree is known, the varying curve of permittivity and conductivity could be modified. However, the modification of dielectric properties is only limited to the location where dielectric property begins to change. In Fig. 4, heterocharge "6" and "9" could also be observed near the anode. Negative charge "8," "11" and "13" could be observed at the anode; this is regarded as the induced charge of the homocharge accumulated in the water tree area. The presence of the negative induced charge explains why the amplitude of induced charge peaks in anode is found smaller for water-aged cables among all groups in Fig. 3.


FIGURE 5. Space charge distribution of unaged (a, b, c) and water-aged (d, e, f) cables during the depolarization process and after application of the subtraction method to the polarization process data obtained at 20 kV/mm.

Fig. 5 shows the space charge distribution of unaged (a, b, c) and water-aged (d, e, f) cables during the depolarization process and after application of the subtraction method to the polarization process data obtained at 20 kV/mm. By comparing the profile of the depolarization conducted at 60 s/1800 s and the profile obtained after applying the subtraction method with the polarization process data obtained at 20 kV/mm, we deduce that shallow trap space charge exists. The shallow trap charge escapes quickly when the depolarization process begins, even when the applied

voltage begins to decrease. Fig. 5 shows that the space charge that finally remains is deep trapped charge, indicating that both shallow and deep traps exist in the water tree area. Based on comparison of the data for the unaged and water-aged cables shown in Fig. 3, Fig. 4, and Fig. 5, we deduce that a wide range of positive charges accumulates in the insulation of water-aged cables. This indicates that large numbers of traps and ions are present in the insulation after the water-aging process.

After the space charge measurements of the cables were obtained, the measurement points were marked. Insulation slices along the radial direction of the cable were then prepared, and the water tree could be determined outside the insulation after the dyeing process. This verifies that the injected positive charges observed in the experiments are caused by the water tree.
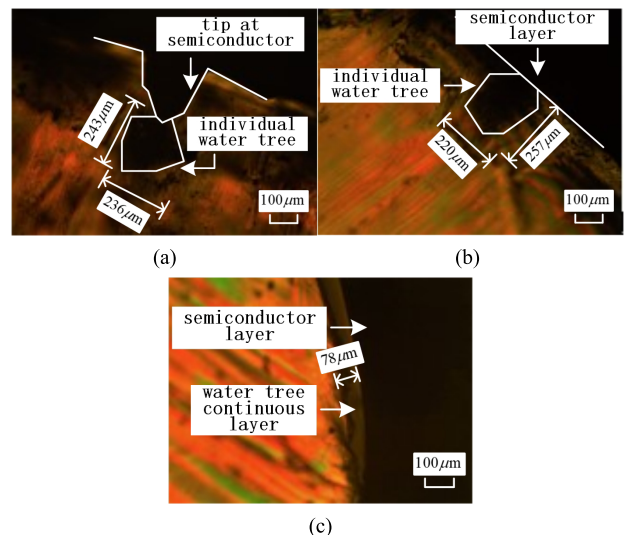
FIGURE 6. Water trees observed microscopically at 200x magnification. (a) AW cable. (b) BW cable. (c) CW cable.

The water tree observation results of aged samples are shown in Fig. 6. The water trees in AW and BW cables are individual water trees, and the water tree in CW is a continuous water tree layer.

B. SIMULATION RESULTS
In the simulation, the length of the vented tree is $300\mu m$. The other cable geometry parameters refer to actual parameters. The inner radius of the insulation is 7 mm, and its outer radius is 11.5 mm. The voltage also refers to the experiment; a negative voltage with an average electric field of 10, 15, and 20 kV/mm is applied to the conductor. The insulation is divided equally into 500 elements; the time-step is 0.05 s. The results obtained by simulation of the space charge distribution of water-aged cables with electric fields at 10, 15, and 20 kV/mm are shown in Fig. 7.

The PEA measurement signal in the oscilloscope is recorded according to the distance from the acoustic transducer. Although the waveform obtained in the experiment
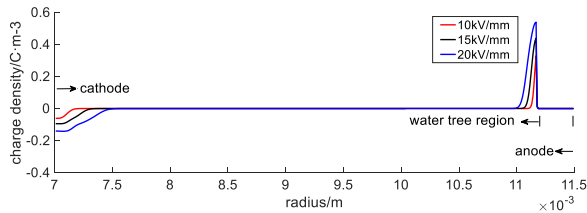
FIGURE 7. Simulation of the space charge distribution of water-aged cables with electric fields of 10, 15, and 20 kV/mm.

appears opposite to the waveform obtained in the simulation, they are actually exactly consistent.

If the forward Euler method used in previous algorithm is adopted in this paper to separate the charge conservation equation in time domain, the time step will be limited by CFL condition, $\Delta t < \Delta x/(wn)$, where Δx is the element length, w is the velocity of charge, n is the charge density. According to the value in this paper, the time step is very small as $1\mu s$. Thus the efficiency of the modified algorithm over the previous one is greatly improved.

Note that in the simulation, the electric field near both anode and cathode are judged before each calculation loop. Only when the electric field exceeds the threshold value that the charge injection could happen. The simulation results presented in Fig. 7 show that there is little accumulated charge in the water tree region near the anode under different stress electric fields. Near the tip of the water tree, a large amount of accumulated homocharge is found in the insulation compared with the cathode. The amount of homocharge in the insulation both near the cathode and near the water tree tip increases with DC stress electric field. Both the experimental results and the simulation results show that although the charge moves inside over time and DC stress voltage, the interface of the XLPE insulation and the vented tree does not move; this indicates that the influence of the space charge on the water tree growth under DC stress is not obvious over a short period. By examining the data shown in Fig. 4 on the space charge distribution of the water tree aged cables and by applying the subtraction method to the polarization process data, the simulation results are identical to the experimental results, especially for the water tree region, which is the focus of this study. Thus, the set of algorithms presented here can be used to solve the charge-coupled problem with defects. The simulation results and the experimental results obtained for water-aged insulation differ in two aspects: the width of the charge peak and the charge distribution in the insulation, except in the water tree region. Regarding the width of the charge peak, the width of the experimental peak is obviously larger than that of the simulation peak. The two main reasons for this difference are as follows: first, the resolution ratio of the measurement system is not absolutely ideal; second, the parameters function of the interface may not be absolutely consistent with the practical conditions. For the charge distribution in the insulation excepting the water tree region, specific characteristics of the materials or the

manufacturing technique used could lead to charge accumulation. As mentioned in Section II, the model does not consider ionic charges to clearly reveal the influence of the injected charges in the water tree region, and this may also result in a difference between the simulated results and the experimental results. In the following studies, these two aspects of the model will be improved to better simulate the space charge behavior of the entire cable insulation.

V. DISCUSSION
A. CHARACTERISTICS OF DIELECTRIC PARAMETERS AT THE INTERFACE REGION

One key point in the algorithm that requires further discussion is whether the assumption of the dielectric parameters function is consistent with the practical conditions. Although the suitability of the assumption could be verified by a comparison of the simulated results with the experimental results, it is still essential to consider the distribution of the dielectric parameters from a microscopic perspective.

Water trees have been thoroughly studied with the aid of various techniques, such as FTIR and optical and electron microscopy, revealing their structure. The structure comprises a multitude of water-filled microcavities that might contain various amounts of conductive impurities or other contaminants. Since it is likely that the microcavities diffuse into the healthy XLPE insulation, which means that the number of cavities decreases from the water tree tip to the insulation, it is rational to assume that the conductivity or the permittivity changes monotonically. In this paper, using the results of previous research [28] as a reference, both conductivity and permittivity change in an exponential manner.

As shown in Fig. 4, the space charge accumulation in the water tree region is not a linear function of the electric field. The structure of water tree consists of voids with interlinking channels. These interlinking channels are considered not fully open under low electric field. As the electric field increases to a certain extern, the interlinking channels gradually opens caused by Maxwell forces. Thus, the conductivity of water tree is enhanced under high electric field. This indicates that the dielectric parameters may display a nonlinear relationship in high electric fields. For this purpose, a nonlinear relationship should be considered in subsequent research; this might further improve the accuracy of the simulation.

B. SPACE CHARGE BEHAVIOR AT THE WATER TREE REGION

According to previous research [29], [30], two main types of charges are present in XLPE insulation containing water trees: one is ionic charge ionized from hydrates or impurities, which could appear under very low electric fields and disappear during depolarization; another type of charge is charge injected from the water tree tip to the insulation at higher electric fields, which still exists even after depolarization. Since the conductivity of water tree is quite high,

the injected charge moves quickly to water tree tip. Thus, no charge is observed on the anode electrode. Thus, in PEA measurement results, it could be regarded that injected charge peak on the electrode shift to water tree tip. Considering the process that charge transports into XLPE insulation from water tree tip, charge hops between trap sites in insulation instead of transporting freely. The hop behavior limited by a potential barrier, which could be lower by an applied electric field.

The cables studied in this paper were water-aged for a long time. The water that intruded into the insulation induced the formation of vented trees near the outer semiconductor layer. The space charge accumulated at the microcavities of the tree tip and was injected into the insulation. Homocharge accumulation near the electrodes is usually believed to be caused by charge injection at the electrodes, whereas heterocharge may be formed in two ways: 1) field assisted ionic dissociation of chemical species intrinsic to the insulation; 2) injected charge blocked or partly blocked at the counter electrode [19]. The experimental results show that two kinds of charges exist, as shown in Fig. 5. Thus, after validating the feasibility and accuracy of the modified algorithm by simulating the injected charge in the water tree, the influence of ionic charge will be considered in the following research.

In this paper, the combination of the bipolar model and the functionalization of the dielectric parameters represents a novel attempt to describe charge behavior in insulation with defects. The method presented is applicable to an interface that is not instantaneous but diffuse. For such a problem, the Maxwell-Wagner model could not be simply employed as a solution, nor could it describe the charge injection or the influence of the surface state. Furthermore, the application of the Crank-Nicolson algorithm in this model overcomes the time-step limitation, facilitating the solution of problems involving defects that give rise to large conductivities. According to our research, certain aspects of this algorithm need to be improved for further practical engineering application. As mentioned above, the nonlinear characteristics of dielectric parameters under a high electric field, a condition that may not occur under working conditions but is very common in laboratory studies, should be considered. In the following research, this model will also be applied to insulation that contains bow-tie water trees or other defects. The model is most suitable for charge behavior simulation during the PEA measurement procedure under DC voltage stress. When applying this model to charge behavior simulation under practical working conditions, two main challenges arise. One is that the mutual influence between space charge and water tree development should be considered during long-term simulations; this might require the use of a time-varying function to replace the present dielectric parameter function. The other challenge is that the voltage stress should be set according to the practical conditions (AC, DC, or superposition of voltages of different frequencies). In addition, the simulation parameters must reflect real charge behaviors under different voltage types.

VI. CONCLUSION

This paper presents details of the development of a modified bipolar charge transport model that can be used to explain the process of charge formation in water tree aged cable insulation. The model takes into account the dielectric properties of the corresponding water tree areas and the cylindrical geometry. The conclusions of this paper are as follows:

1) A diffuse interface between water trees and healthy insulation could be modeled as a function of the dielectric parameters, and this could be combined with the bipolar model to solve the charge-coupling problem.
2) The use of the Crank-Nicolson method effectively overcomes the time-step limitation and greatly improves simulation efficiency.
3) By adopting the subtraction method near the interface between the water tree and healthy insulation, charges trapped in both shallow and deep traps are found in PEA measurements.
4) Whereas the charge moves inside over time under the influence of a DC stress voltage, the interface of the XLPE insulation and the vented tree does not move under DC stress in a short period.

In conclusion, the model describes the behavior of space charge in insulation with water tree defects of cylindrical geometry. However, as mentioned above, some improvements are needed.

REFERENCES

[1] G. Mazzanti and M. Marzinotto, "Fundamentals of HVDC cable transmission," in *Extruded Cables for High-Voltage Direct-Current Transmission: Advances in Research and Development*, 1st ed., J. Anderson, Ed. Hoboken, NJ, USA: Wiley, 2013, pp. 11–40.

[2] K. Uchida *et al.*, "Study on detection for the defects of XLPE cable lines," *IEEE Trans. Power Del.*, vol. 11, no. 2, pp. 663–668, Apr. 1996.

[3] W. Li *et al.*, "Frequency dependence of breakdown performance of XLPE with different artificial defects," *IEEE Trans. Dielectr. Electr. Insul.*, vol. 19, no. 4, pp. 1351–1359, Aug. 2012.

[4] K. Zhou, M. Huang, W. Tao, M. He, and M. Yang, "A possible water tree initiation mechanism for service-aged XLPE cables: Conversion of electrical tree to water tree," *IEEE Trans. Dielectr. Electr. Insul.*, vol. 23, no. 3, pp. 1854–1861, Aug. 2016.

[5] K. W. Burkes, E. B. Makram, and R. Hadidi, "Water tree detection in underground cables using time domain reflectometry," *IEEE Power Energy Technol. Syst. J.*, vol. 2, no. 2, pp. 53–62, May 2015.

[6] P. Werelius, P. Tharning, R. Eriksson, B. Holmgren, and U. Gafvert, "Dielectric spectroscopy for diagnosis of water tree deterioration in XLPE cables," *IEEE Trans. Dielectr. Electr. Insul.*, vol. 8, no. 1, pp. 27–42, Mar. 2001.

[7] A. Ponniran and M. Kamarudin, "Study on the performance of underground XLPE cables in service based on tan delta and capacitance measurements," in *Proc. IEEE Int. Conf. Power Energy (ICPE)*, Johor Bahru, Malaysia, Dec. 2008, pp. 39–43.

[8] M. Abou-Dakka, A. Bulinski, and S. S. Bamji, "On-site diagnostics of medium-voltage underground cross-linked polyethylene cables," *IEEE Elect. Insul. Mag.*, vol. 27, no. 4, pp. 34–44, Jul. 2011.

[9] M. J. Given, R. A. Fouracre, S. J. MacGregor, M. Judd, and H. M. Banford, "Diagnostic dielectric spectroscopy methods applied to water-treed cable," *IEEE Trans. Dielectr. Electr. Insul.*, vol. 8, no. 6, pp. 917–920, Dec. 2001.

[10] Y. Yagi, H. Tanaka, and H. Kimura, "Study on diagnostic method for water treed XLPE cable by loss current measurement," in *Proc. IEEE Conf. Electr. Insul. Dielectr. Phenom. (CEIDP)*, Atlanta, GA, USA, Oct. 1998, pp. 653–656.

[11] C. Parkey, C. Hughes, and N. Locken, "Analyzing artifacts in the time domain waveform to locate wire faults," *IEEE Instrum. Meas. Mag.*, vol. 15, no. 4, pp. 221–225, Aug. 2011.

[12] Y. Li *et al.*, "Space charge behavior under ac voltage in water-treed PE observed by the PEA method," *IEEE Trans. Dielectr. Electr. Insul.*, vol. 4, no. 1, pp. 52–57, Feb. 1997.

[13] K. Suzuki, Y. Tanaka, T. Takada, Y. Ohki, and C. Takeya, "Correlation between space charge distribution and water-tree location in aged XLPE cable," *IEEE Trans. Dielectr. Electr. Insul.*, vol. 8, no. 1, pp. 78–81, Mar. 2001.

[14] A. J. Thomas and T. K. Saha, "A new dielectric response model for water tree degraded XLPE insulation—Part A: Model development with small sample verification," *IEEE Trans. Dielectr. Electr. Insul.*, vol. 15, no. 4, pp. 1131–1143, Aug. 2008.

[15] A. J. Thomas and T. K. Saha, "A new dielectric response model for water tree degraded XLPE insulation—Part B: Dielectric response interpretation," *IEEE Trans. Dielectr. Electr. Insul.*, vol. 15, no. 4, pp. 1144–1152, Aug. 2008.

[16] L. Hui, L. S. Schadler, and J. K. Nelson, "The influence of moisture on the electrical properties of crosslinked polyethylene/silica nanocomposites," *IEEE Trans. Dielectr. Electr. Insul.*, vol. 20, no. 2, pp. 641–653, Apr. 2013.

[17] J. M. Alison and R. M. Hill, "A model for bipolar charge transport, trapping and recombination in degassed crosslinked polyethene," *J. Phys. D, Appl. Phys.*, vol. 27, no. 6, pp. 1291–1299, 1994.

[18] S. Le Roy, G. Teyssèdre, and C. Laurent, "Modelling space charge in a cable geometry," *IEEE Trans. Dielectr. Electr. Insul.*, vol. 23, no. 4, pp. 2361–2367, Aug. 2016.

[19] L. Lan, J. Wu, Y. Yin, and Q. Zhong, "Investigation on heterocharge accumulation in crosslinked polyethylene: Experiment and simulation," *Jpn. J. Appl. Phys.*, vol. 53, no. 7, p. 071702, Jun. 2014.

[20] T. Toyoda, S. Mukai, Y. Ohki, Y. Li, and T. Maeno, "Estimation of conductivity and permittivity of water trees in PE from space charge distribution measurements," *IEEE Trans. Dielectr. Electr. Insul.*, vol. 8, no. 1, pp. 111–116, Mar. 2001.

[21] Y. Zhang, K. Qian, J. Wu, and Y. Yin, "Assessment of 10kV HVAC cable under different aging modes by pulsed electro-acoustic method," in *Proc. IEEE Conf. Condition Monitor. Diagnosis (CMD)*, Xi'an, China, Sep. 2016, pp. 964–967.

[22] J. Wu, "Charge transport investigation in low-density polyethylene/silica nanocomposite based on experiment on numerical simulation," (in Chinese), Ph.D. dissertation, School Electron. Inf. Elect. Eng., Shanghai Jiao Tong Univ., Shanghai, China, 2012.

[23] Y. Ohki, Y. Ebinuma, and S. Katakai, "Space charge formation in water-treed insulation," *IEEE Trans. Dielectr. Electr. Insul.*, vol. 5, no. 5, pp. 707–712, Oct. 1998.

[24] R. I. Mclachlan and G. R. W. Quispel, "Splitting methods," *Acta Numer.*, vol. 11, pp. 341–434, Jan. 2002.

[25] J. Crank and P. Nicolson, "A practical method for numerical evaluation of solutions of partial differential equations of the heat-conduction type," *Adv. Comput. Math.*, vol. 6, no. 1, pp. 207–226, Jun. 1996.

[26] G. C. Montanari, C. Laurent, G. Teyssedre, A. Campus, and U. H. Nilsson, "From LDPE to XLPE: Investigating the change of electrical properties. Part I. Space charge, conduction and lifetime," *IEEE Trans. Dielectr. Electr. Insul.*, vol. 12, no. 3, pp. 438–446, Jun. 2005.

[27] N. Liu, C. Zhou, G. Chen, and L. Zhong, "Determination of threshold electric field for charge injection in polymeric materials," *Appl. Phys. Lett.*, vol. 106, no. 19, p. 192901, May 2015.

[28] J. Bezille, H. Janah, J. Chan, and M. D. Hartley, "Influence of diffusion on some electrical properties of synthetic cables," in *Proc. IEEE Conf. Electr. Insul. Dielectr. Phenom. (CEIDP)*, Victoria, BC, Canada, Oct. 1992, pp. 367–372.

[29] Y. Li *et al.*, "Three-dimensional space charge distribution in water tree tip using the pulsed electroacoustic method," in *Proc. IEEE Int. Symp. Dielectr.*, Shanghai, China, Sep. 1996, pp. 217–222.

[30] C. Stancu *et al.*, "Computation of the electric field in cable insulation in the presence of water trees and space charge," *IEEE Trans. Ind. Appl.*, vol. 45, no. 1, pp. 30–43, Jan. 2009.
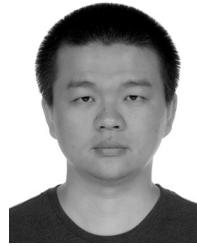
YU ZHANG was born in Zhejiang, China, in 1991. He received the B.Eng. degree from Xi'an Jiao Tong University, Xi'an, in 2014. He is currently pursuing the Ph.D. degree with Shanghai Jiao Tong University. His research interest is the simulation of charge transport in polymeric insulation systems.

DEYUAN LIU was born in Harbin, China, in 1994. He received the B.Eng. degree from Shanghai Jiao Tong University, Shanghai, in 2016, where he is currently pursuing the M.E. degree. His research interest is the dielectric properties of polymeric insulation materials.

JIANDONG WU (M'13) received B.Sc. and M.E. degrees from Southwest Jiao Tong University, China, in 2005 and 2008, respectively, and the Ph.D. degree in electrical engineering from Shanghai Jiao Tong University in 2012. From 2010 to 2011, he was an Assistant Researcher with the Tanaka's Laboratory, IPS Center, Waseda University, Japan. From 2014 to 2016, he was a Post-Doctoral Research Fellow with Shanghai Jiao Tong University. During this period, he visited the University of Southampton for one year as a Visiting Academic. He is currently with Shanghai Jiao Tong University as an Associate Professor. His research interests are space charge detecting and simulation technologies for electrical insulation.

YI YIN (M'13) was born in Jiangsu province, China, in 1972. He received the B.Sc., M.E., and Ph.D. degrees in electrical engineering from Xi'an Jiao Tong University, China, in 1994, 1997, and 2000, respectively. In 2000, he moved to Shanghai Jiao Tong University, China. Since 2009, he has been a Professor with Shanghai Jiao Tong University. He has worked on electrical aging of polymer insulating materials, dielectric properties of polymer nanocomposites, and monitoring on-line of power apparatus.

• • •